



HAL
open science

Multi-scale experimental investigation of the viscous nature of damage in Advanced Sheet Molding Compound (A-SMC) submitted to high strain rates

Mohammadali Shirinbayan, Joseph Fitoussi, Michel Bocquet, Fodil Meraghni, Benjamin Surowiec, Abbas Tcharkhtchi

► To cite this version:

Mohammadali Shirinbayan, Joseph Fitoussi, Michel Bocquet, Fodil Meraghni, Benjamin Surowiec, et al.. Multi-scale experimental investigation of the viscous nature of damage in Advanced Sheet Molding Compound (A-SMC) submitted to high strain rates. *Composites Part B: Engineering*, 2017, 115, pp.3-13. 10.1016/j.compositesb.2016.10.061 . hal-01540457

HAL Id: hal-01540457

<https://hal.science/hal-01540457>

Submitted on 10 Jul 2017

HAL is a multi-disciplinary open access archive for the deposit and dissemination of scientific research documents, whether they are published or not. The documents may come from teaching and research institutions in France or abroad, or from public or private research centers.

L'archive ouverte pluridisciplinaire **HAL**, est destinée au dépôt et à la diffusion de documents scientifiques de niveau recherche, publiés ou non, émanant des établissements d'enseignement et de recherche français ou étrangers, des laboratoires publics ou privés.

Multi-scale experimental investigation of the viscous nature of damage in Advanced Sheet Molding Compound (A-SMC) submitted to high strain rates

M. Shirinbayan ^{a, *}, J. Fitoussi ^a, M. Bocquet ^a, F. Meraghni ^b, B. Surowiec ^c, A. Tcharkhtchi ^a

^a Arts et Métiers ParisTech, PIMM – UMR CNRS 8006, 151 Boulevard de l'Hôpital, 75013 Paris, France

^b Arts et Métiers ParisTech, LEM3 – UMR CNRS 7239, 4 Rue Augustin Fresnel, 57078 Metz, France

^c Plastic Omnium Auto Exterior, Sigmatech, Sainte Julie, France

A B S T R A C T

This paper aims to present an experimental multi-scale analysis of quasi-static and high strain rate damage behavior of a new formulation of SMC composite (Advanced SMC). In order to study its capability to absorb energy through damage accumulation, Randomly Oriented (RO) and High oriented (HO) A-SMC composites damage has been investigated at both microscopic and macroscopic scales. A specific device has been developed in order to perform Interrupted Dynamic Tensile Tests (IDTT) which allows analyzing the evolution of the microscopic damage mechanisms occurring during rapid tensile tests. Several damage micro-mechanisms have been pointed out. The relative influences of these micro-damage events and their interactions have been related to the macroscopic damage behavior through the definition of microscopic and macroscopic damage indicators. Damage threshold and kinetic have been quantified at various strain rate for different microstructures and loading cases (RO, HO-0° and HO-90°). It has been shown at both scales that increasing strain rate leads to an onset of damage initiation together with a reduction of the damage accumulation kinetic. Moreover, the influence of the fiber orientation has been studied in order to emphasize the anisotropic strain rate effect at the fiber-matrix interface scale. The latter was related to the influence of the microstructure of A-SMC composites. Finally, on the basis of the whole experimental results, the microscopic origin of the viscous nature of the damage behavior of A-SMCs composites have been discussed and related to the influence of the strain rate and microstructure.

1. Introduction

Because of their high energy absorption capacity, short fiber reinforced composite materials are often used for automotive structures submitted to crash events. In contrast to metallic materials for which energy absorption is provided by plastic deformation [1], composites material structures crashworthiness mostly consists of several diffuse and progressive damage mechanisms occurring at the local scale such as matrix micro-cracking [2], fiber failure [3], debonding at the fiber-matrix interface [4–6], delamination or pseudo-delamination [7]. This is an extremely important issue for automotive industry. Indeed, local damage development

allows composite structures to absorb significant impact energy in such a way that the progressive degradation enables to minimize the transmitted energy to passenger and to assure his safety. On the other hand, several earlier studies [8,9] have shown that the energy absorption capacity of polymers and composites materials is highly dependent on the microstructure parameters such as fiber content, type of fiber and matrix or fiber orientation and length. Furthermore, a good crashworthiness requires avoiding damage localization leading to a brittle failure and limited absorbed energy. So, in order to favor a diffuse damage development, a better understanding of the damage mechanisms which can occur during high strain rate loading is required.

Composite design capable of good crash resistance requires acquiring a thorough knowledge of its capacity to develop damage phenomenon [10,11]. However, short fiber reinforced composite structure design is in general a difficult challenge because of several specificities such as the variability of the microstructure [7], the anisotropic behavior [12], multiple coupled damage mechanisms

which produce an evolution of the anisotropy during loading [13] etc. A lack of unawareness regarding the influence of high loading rate on the local damage mechanisms could lead to a less effective composite structure design. In particular with regard to the choice of damage behavior laws used in finite element calculations for crashworthiness design, the influence of microstructure parameters and strain rate on the threshold and kinetic of damage is of prime importance. Indeed, when damage behavior of composite materials is analyzed especially at different strain rate, the architecture (Orientation of reinforcements, laminate) and the matrix behavior (Elastic, visco-elastic, visco-plastic) should be considered. Thermoplastic [14] and thermoset materials [7] have different damage behavior subjected to loading at different strain rate.

Several studies have proposed models to account for the damage behavior of composite and specific implementation techniques for numerical simulations have been developed [15–17]. One may distinguish two kind of predictive modeling of composite material behavior: phenomenological and micro-mechanical approach. For both approach, damage variables are described. For the micro-mechanical approach these variables describe the evolution of the micro-cracks content during loading [18–21]. The phenomenological approach aims to describe the consequence of the local damage at the macroscopic scale such as loss of stiffness. In this approach, the macroscopic scale corresponds to the Representative Volume Element (RVE) of composite material. However, to make easy the micro-mechanical calculations, the damage variable is sometimes non-local [22]. In this case, the crack data are usually homogenized. This approach is often adopted in mixed models of damage, combining micro-mechanical and phenomenological aspects [23]. Conversely, in energy approaches, the damage variable is mostly unrelated to the physical reality [24]. Most damage models can represent a softening deformation [25]. Mixed models are most often associated with a fracture criterion [26]. In phenomenological models, mechanical behavior laws are derived from thermodynamic potentials and the representation of the mechanical degradation is more finite [18]. Damage phenomenological models can be used more easily than the micro-mechanical damage models in numerical simulation, because energy formulations do not need the microscopic data [18,19]. On the other hand, in micro-mechanical models, the damage variable has a physical sense related to the volume fraction occupied by cracks in the damaged composite, the rate of energy dissipated by fracture or cracks parameters [20,21].

Moreover, especially with regard to the anisotropy evolution due to damage observed in the short fiber reinforced composite [13], the micromechanical modeling seems to be a more suitable approach for the prediction of the behavior and damage of this class of materials. In these models, damage can be taken into account through several local damage criterions which are in competition and determine the introduction of micro-cracks at the local scale [27–29].

One can conclude that, whatever the numerical approach used, a thorough knowledge of the type of local damage mechanisms, their threshold and kinetic is always needed on one hand for the choice of a suitable damage behavior law and for the identification of its variables on the other hand [28–30].

The purpose of this study concerns a new formulation of SMC composite which have recently be developed: A-SMC. Advanced Sheet Molding Compound (A-SMC) is a high performance SMC composite based on vinylester resin and reinforced with 50% (in mass) of chopped bundles of glass fibers [7]. A-SMCs are provided by Plastic Omnium Auto Exterior and are processed by thermo-compression [7]. These composites are commonly used as a substitute for steels in structural automotive components because of their high strength-to-weight ratio [31,32]. A recent study [7] have demonstrated their high stiffness and strength together with low

density compared to metals which make them suitable materials for crashworthy small weight automotive structures. This paper aims to the determination of the damage mechanisms and their influence on the macroscopic response of A-SMC composites when they are submitted to high strain rates.

Different experimental techniques characterize the damage at macroscopic and microscopic scales: Loading unloading at different loading directions, acoustic emission technique [33], in-situ SEM microscopy testing [5] and also micro-tomography X method [29], anisotropic stiffness reduction measurement by ultrasonic technique and etc [13]. In the case of dynamic loading, it is not possible, because of uncontrolled inertial effect, to measure the stiffness reduction by loading-unloading tests. Likewise, the micro-scale monitoring of the damage phenomenon is difficult. In this study, the methodology of interrupted tests already used in the case of standard SMC and PP composite [4,5] will be illustrated in the case of A-SMC. In these previous studies, the experimental results showed that the predominant damage mechanism is the fiber-matrix interface debonding. However, micro-cracking of the matrix can also play a significant role in particular during the last stages before failure through the coalescence of the fiber-matrix interface micro-cracks across the matrix. It has been shown that, for a standard SMC, when the strain rate increases, a delayed damage onset is followed by a reduction damage accumulation kinetic.

Several studies show that the mechanical response of A-SMC and also SMC composites is strongly dependent on the micro-structure variability and strain rate [4–7]. A micro-mechanical model based on a statistical local interface failure criterion introduced in the Mori and Tanaka model was earlier proposed by Fitoussi [6], in order to predict the tensile curves and the stiffness reduction due to damage for SMC composite. This kind of micro-mechanical model was introduced in a finite element analysis for composites structure damage analysis by Derrien et al. [34] and Meraghni et al. [35]. This approach was validated in the case of bending-torsion test. Jendli et al. [12] have generalized this approach to high strain rate loading. They used the multi-scale experimental analysis of high strain rate interrupted tensile tests [5] to identify and validate a multi-scale visco-damageable model [27].

In the present paper, we apply the method of interrupted tensile test to identify damage mechanisms (Damage thresholds and kinetic) depending on the orientation of reinforcements and strain rate in order to make the database needed to built a predictive model of the micro-mechanical behavior of A-SMC under crash loading.

The organization of this paper is as follow: A-SMC composite composition and two kind of this composite (Randomly Oriented (RO) and Highly Oriented (HO) plates) provided by Plastic Omnium Auto Exterior are introduced in material specification section. In the case of HO samples, two tensile directions were selected in order to evaluate the anisotropic effect due to microstructure: HO-0° (parallel to the Mold Flow Direction (MFD)) and HO-90° (perpendicular to the MFD). Quasi-static tensile tests with damage evolution at macroscopic scales are investigated for HO samples. Subsequently, the results of low and high strain rate tensile test until failure and damage evolution at macroscopic and microscopic scales for RO samples are presented. The visco-damageable behavior of A-SMC composites is correlated to observations performed at the local scale. The effect of high strain rate on elastic properties, damage threshold and kinetic are analyzed at both microscopic and macroscopic scale. A previous work [5] showed that, depending on microstructure and strain rate, the development of a pseudo-delamination stage between bundles of fibers which can occur before failure. At the end of this paper, SEM analysis emphasizes the effect of strain rate on the pseudo-delamination.

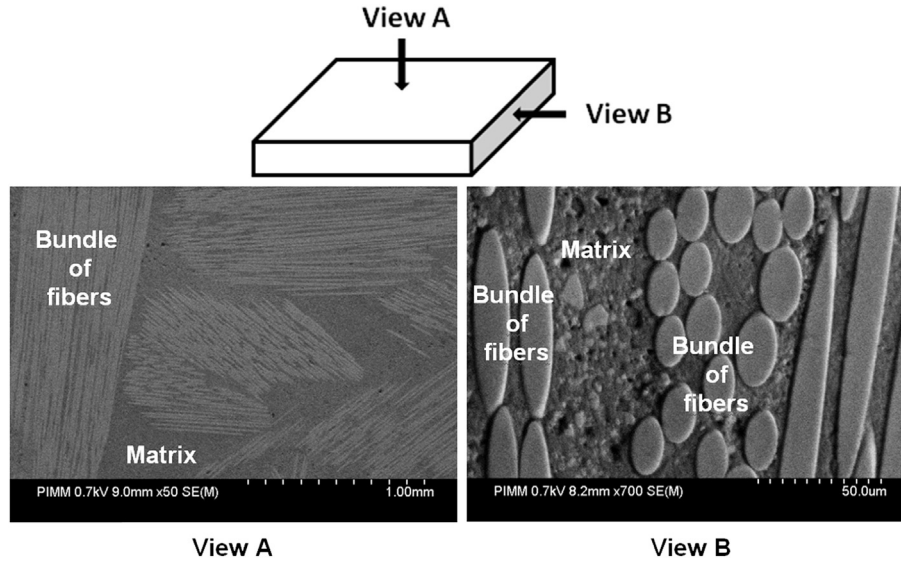


Fig. 1. Microstructure of RO-A-SMC composite.

2. Material specification and methods

2.1. Advanced Sheet Molding Compound (A-SMC) composite

Advanced Sheet Molding Compound (A-SMC) composite is typically used in automotive industry. A-SMC is a high mechanical performance SMCs consisting of a vinyl-ester resin reinforced by a high content of chopped bundles of glass fibers (50% in mass corresponding to 38.5% in volume). Two types of A-SMC plates have been provided by Plastic Omnium Auto Exterior: Randomly Oriented (RO) and Highly Oriented (HO) plates. HO plates have been obtained by placing the initial charge of SMC prepreg sheets only in the left part of a rectangular mold ($30 \times 40 \text{ cm}^2$). Thus, compression molding leads to material flow and fiber orientation. RO plates were obtained without material flow by completely filling the mold. Fig. 1 shows microstructure of A-SMC observed by SEM microscope on polished surfaces. Indeed, fibers are initially randomly oriented in the SMC prepreg sheets before compression. The fibers are presented as bundles of constant length ($L = 25 \text{ mm}$). Each bundle contains approximately 250 fibers of $15 \mu\text{m}$ diameter.

2.2. Methods

In order to study the damage behavior of A-SMC composite, interrupted high speed tensile test at different strain rate have been performed and deeply analyzed at both microscopic and macroscopic scales on Randomly Oriented (RO) plates. Moreover, in the case of HO plates, two tensile directions; HO- 0° (parallel to the Mold Flow Direction (MFD)) and HO- 90° (perpendicular to the MFD) were used to investigate the damage behavior in quasi-static tensile test.

2.2.1. Low and high speed tensile tests

Low-speed tensile tests and also quasi-static loading-unloading tensile tests have been performed at different defined maximum stress using a MTS 830 hydraulic machine. The analysis of the reloading slope leads to the determination of the loss of stiffness (see equation (1) in section 3.3).

At the other hand, a servo-hydraulic machine as specified by the manufacturer (Schenk Hydroluls VHS 5020) was used to perform tensile tests at different strain rates from quasi-static to 60 s^{-1} . The A-SMC sample is positioned between the load cell (upper

extremity) and the moving device (lower extremity) as shown in Fig. 3(a). In order to get a constant strain rate from the beginning of the high speed tensile test, a tube-piston device allows applying a displacement of the moving device without loading during the acceleration stage.

2.2.2. Interrupted high-velocity tensile test

In order to identify the damage mechanisms occurring during dynamic loading, it is necessary to perform experimental investigations at both macroscopic and microscopic scale. To that end, rectangular specimens with polished surfaces which enable microscopic SEM observations were used as drawn in Fig. 2.

Interrupted high-strain rate tensile test have been originally proposed by Lataillade et al. [36] in the case of glass fiber epoxy laminates. Fitoussi et al. used it for standard SMC composites, carbon Epoxy laminate [5] and short glass fiber reinforced polypropylene [4]. On one hand, this test aims to identify damage mechanisms occurring progressively at the microscopic scale. On the other hand it allows determining the progressive loss of stiffness due to damage. The threshold and kinetic of damage are determined and correlated at both microscopic and macroscopic scale. In this paper, the interrupted dynamic tensile test was developed for A-SMC composite. IDTT is a dynamic loading-unloading test which allows producing successive damaged samples states obtained at different force levels during high-speed loading. The same sample is used several times for increasing levels of applied force. Moreover, before each reloading stage, Scanning Electronic Microscope observations (HITACHI 4800 SEM) have been performed on the polished surface in order to quantify the strain rate effects on the microscopic damage mechanisms (see equations (2) and (3)) in section 3.3 related to the mechanical loss of stiffness of the composite. Thus, A-SMC composites damage was pointed out at two scales (micro and macro).

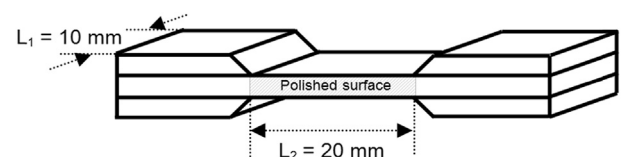


Fig. 2. Rectangular specimen dimension.

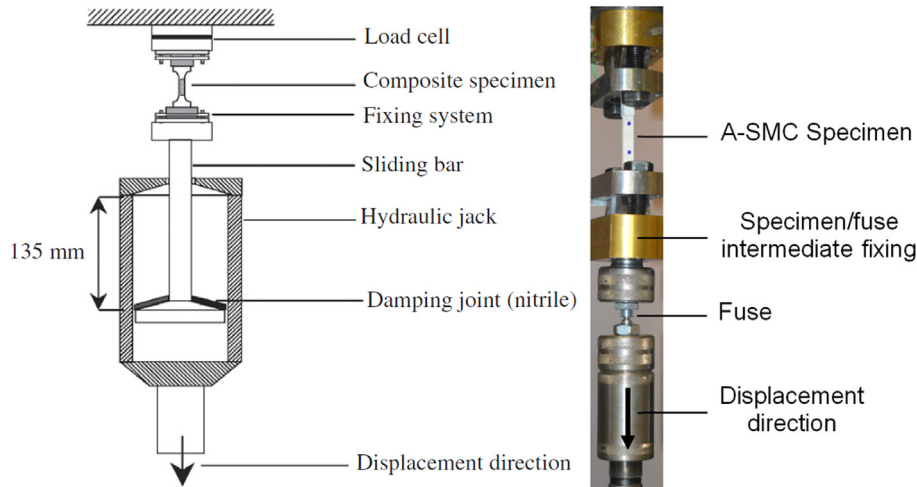


Fig. 3. Interrupted dynamic tensile test: (a) High-strain rate tensile device; (b) Specimen-fuse device for interrupted high-speed tensile test.

The IDTT device is illustrated in Fig. 3(b). During dynamic loading of the sample, the inertia of the hydraulic cylinder, when it is launched, does not allow interrupted test at chosen stress level such as in quasi-static loading-unloading tests. Therefore, the loading of specimen will continue until macroscopic failure. To solve this problem, the basic idea is to place an elastic brittle fuse in series with the composite sample. In this study, a special device was developed and adapted for cylindrical notched steel fuse. The ligament length is related to the maximum value of the required force (see Fig. 7 in section 3.2.2).

2.2.2.1. Fuse characterization. Tensile tests have been performed of the steel fuse for different ligament lengths in order to determine the order of magnitude of the maximum stress. Fig. 4 shows the ultimate force as a function of the fuse ligament length. In fact, the defined force during interrupted high strain rate can be achieved by varying of ligament length. One can note that the ultimate stress can vary for high strain rates. However, no significant variation has been observed during IDTT.

2.2.3. Strain and strain rate measurements

A contactless technique is used to measure the local deformation using a high speed camera (FASTCAM-APX RS). The strain rate measurements procedure has been presented in a previous paper

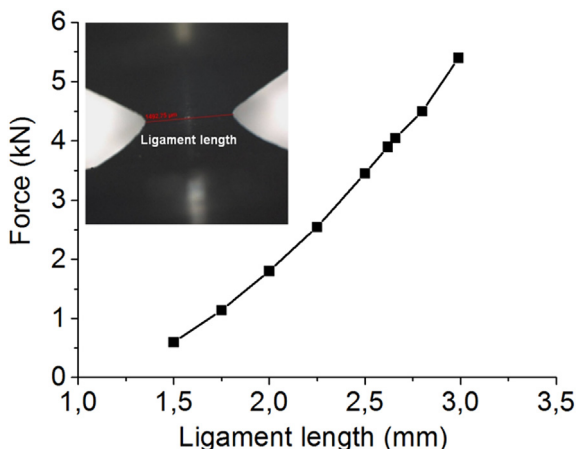


Fig. 4. Required ultimate force as a function of fuse diameter.

[7] and consists in analyzing the images of the filmed surface during deformation.

3. Experimental results and discussion

3.1. Low and high strain-rate tensile test until rupture

In this section, some of the results described in a previous paper [7] are reported in order to justify the choice of the damage experimental analysis presented in this paper.

Quasi-static tensile curves for different fiber direction (HO-90°, RO and HO-0° samples) and the tensile behavior of RO samples at different strain rate of quasi-static, 1 s^{-1} and 60 s^{-1} are presented in Fig. 5(a) and (b), respectively. The material elastic moduli measured in the first stage of the stress-strain curve show a rough average value of 12, 14.5 and 18.5 GPa for HO-90°, RO and HO-0° A-SMCs respectively. However, the non-linear overall response of the A-SMC is obviously clear. These curves are suitable to damage study of different fiber direction.

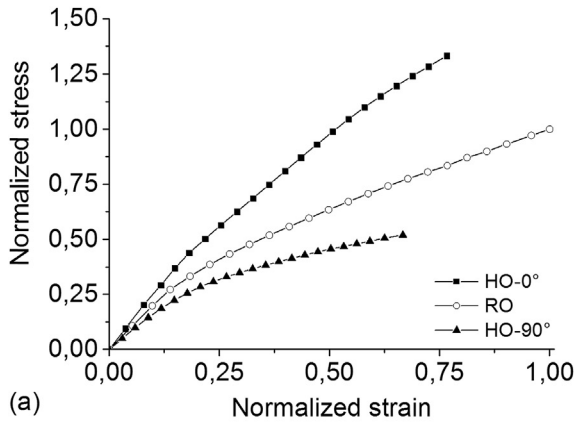
Previous paper [7] indicated that a variation of the strain rate from quasi-static to 60 s^{-1} , lead to an increase of the damage threshold starting from a strain rate of about 1 s^{-1} (Fig. 6). One can note, for RO samples, an increase of 50% of the stress damage threshold and 40% of the ultimate stress when varying the stain rate from the quasi-static to 60 s^{-1} . Therefore, three strain rate ranges were selected for qualitative analysis and quantitative evolution of the damage mechanism of RO samples: quasi-static, 4 s^{-1} and 40 s^{-1} .

3.2. Multi-scale qualitative damage investigation

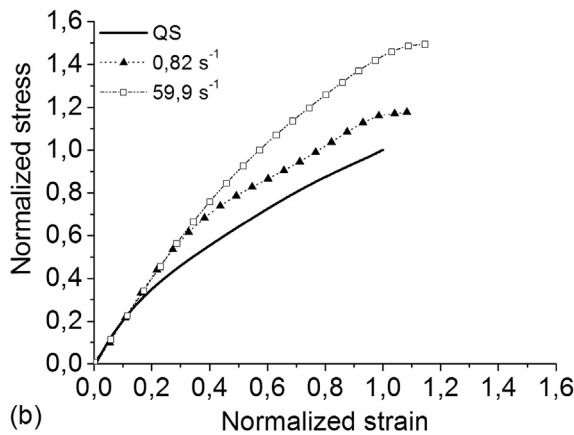
3.2.1. Quasi-static loading-unloading tensile tests

Experimental stress-strain curves for quasi-static loading-unloading tensile test coupled to microstructure observations performed before each reloading stage is shown in Fig. 7.

The same representative observation zone was microscopically analyzed at consecutive increasing value of applied stress level (about $3 \times 5 \text{ mm}^2$). This means that the investigation zone is large enough to contain all the heterogeneities of the material microstructure. The local investigation can be assumed as statistically representative of the damage accumulation in the studied material composite. As mentioned, one must bear in mind that the investigation zone is considered as representative of the material microstructure. In addition, microscopic observations have confirmed the



(a)

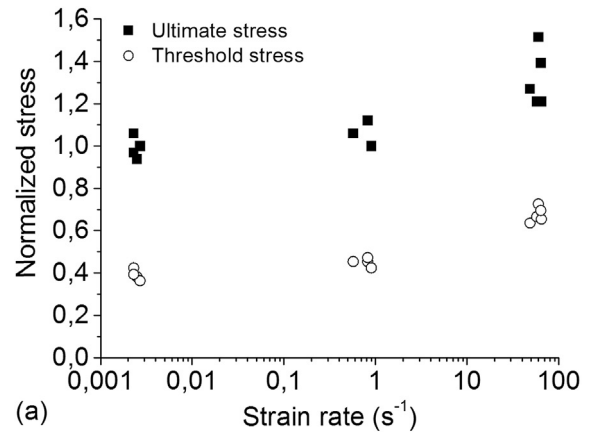


(b)

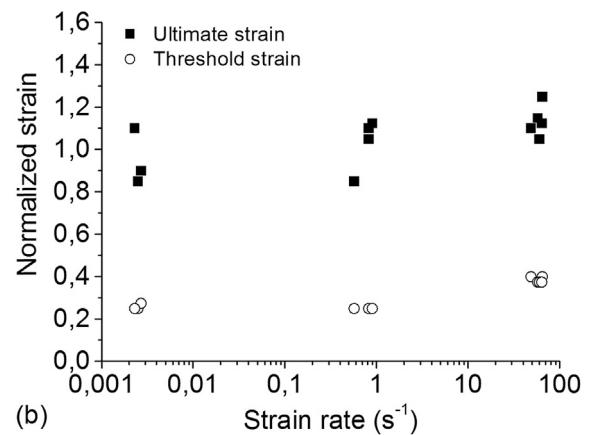
Fig. 5. (a) Normalized quasi-static tensile behavior of A-SMC composites, (b) Normalized tensile curves at different strain rate for RO-A-SMC samples (One can mention that normalized stress (respectively strain) = stress (respectively strain)/ average ultimate stress (respectively strain) obtained for quasi-static tests performed on RO-A-SMC samples used as a reference).

fact that this zone is statistically representative for the damage accumulation.

The first observed damage phenomenon corresponds to the debonding of the fiber-matrix interface. For quasi-static loading, this phenomenon is the predominant damage mechanism. It appears very soon (for 0.35% of σ_r) and propagates through the overall volume of the material as a diffuse manner from the more miss-oriented fibers (90°) to the more oriented fibers (30°). It should be noted that interface debonding is largely favored on the fibers bundles oriented perpendicularly to the principal stress direction. Indeed, these fibers are submitted to a high local normal stress at the interface. Inside each bundle of fibers, fiber-matrix interface failure propagates from one fiber to its neighbor. This phenomenon appears several times on each bundle (from 3 to 5 times) and leads to localized transverse cracks which can be observed in the micrograph performed at an applied stress equal to $0.70 \sigma_r$. Finally, when approaching the ultimate stress, the localized propagate through the matrix located between the bundles and induce pseudo-delamination of the bundles just before final failure. One can conclude that for quasi-static loading, the predominant damage mechanism brings about the diffusion of debonding at the fiber-matrix interface beginning at the more miss-oriented fibers (90°) and progressively diffusing on the less miss-oriented fibers (until 30°). Matrix micro-cracking and pseudo-delamination are secondary damage diffusion mechanisms appearing just before failure. However, they cannot be neglected in the description of the failure process.



(a)



(b)

Fig. 6. Influence of strain rate on: (a) Threshold and ultimate stress, (b) Threshold and ultimate strain (Normalized value = current value/average ultimate value obtained for quasi-static tests performed on RO-A-SMC).

3.2.2. Interrupted high velocity tensile test

Fig. 8 and Fig. 9 show the experimental results of interrupted high strain rate tensile tests performed at 4 s^{-1} and 40 s^{-1} .

The Young's modulus reduction resulting of an increasing applied stress appears clearly and indicates a progressive damage process. At the microscopic scale, one can note debonding at the fiber-matrix interface appearing later than for the quasi-static loading case. This onset of fiber-matrix interface damage increases when increasing strain rate (at $0.45 \sigma_r$ and $0.60 \sigma_r$ for strain rates of 4 s^{-1} and 40 s^{-1} , respectively). On the other hand, one can observe that when increasing the strain rate, the interface damage appears to be less diffuse. Moreover, one can observe that increasing the strain rate favors the propagation of the transverse micro-cracks into the matrix and pseudo-delamination.

3.2.3. Pseudo-delamination mechanism

This phenomenon is called hereafter pseudo-delamination. A previous study [7] showed that, prior to the final failure, local delamination between bundles of fibers always occur independently of the microstructure and strain rate. However, it has been shown that increasing strain rate and orientated fibers favor the pseudo-delamination. Fig. 10 shows a comparison between SEM micrographs performed on RO samples submitted to QS, 4 s^{-1} and 40 s^{-1} . It is obvious to note that in the case of quasi-static loading, pseudo-delamination remains limited while a wide diffuse damage is observed. For higher strain rates, a less diffuse damage and more localized pseudo-delamination is highlighted.

From the overall obtained results of interrupted dynamic tensile tests performed on RO samples, the following conclusions can be

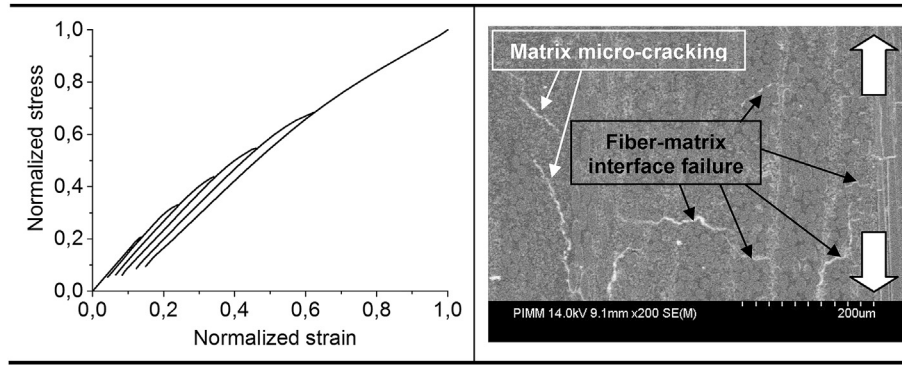


Fig. 7. Damage mechanisms under quasi-static loading unloading tensile test for RO sample (Normalized value = current value/average ultimate stress (σ_r) value obtained for quasi-static tests performed on RO-A-SMC).

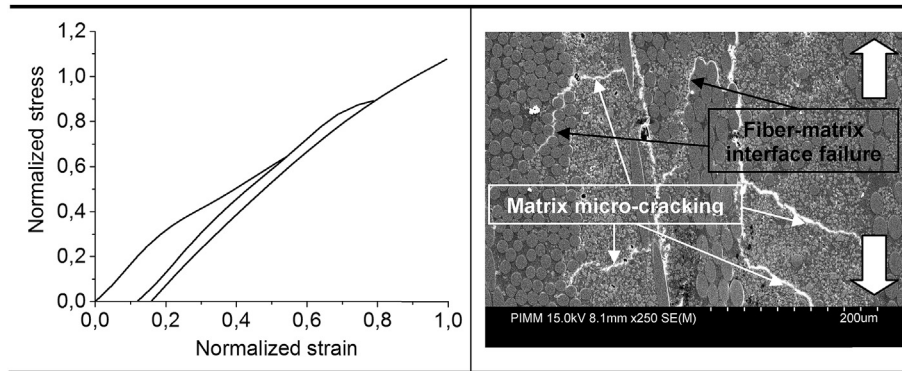


Fig. 8. Damage mechanisms under high strain rate (4 s^{-1}) tensile test for RO sample (Normalized value = current value/average ultimate stress (σ_r) value obtained for quasi-static tests performed on RO-A-SMC).

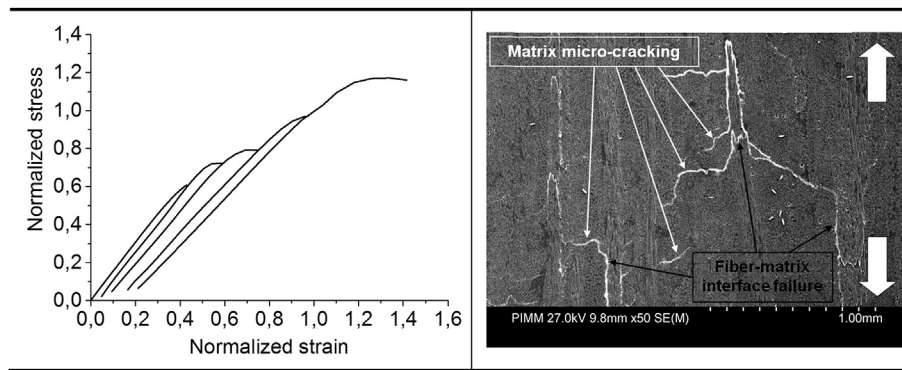


Fig. 9. Damage mechanisms under high strain rate (40 s^{-1}) tensile test for RO sample (Normalized value = current value/average ultimate stress (σ_r) value obtained for quasi-static tests performed on RO-A-SMC).

drawn:

- For both quasi-static and dynamic tests, debonding at the fiber-matrix interface seems to be the predominant diffuse local damage mechanism. Matrix breakage and pseudo-delamination can also appear for higher stress levels.
- When the strain rate increases from quasi-static to 40 s^{-1} , noticeable effect consists of a delayed fiber-matrix damage onset and favored matrix micro-cracking and pseudo-delamination.

3.3. Multi-scale quantitative damage investigation

In this section, a quantitative multi-scale analysis of the damage

effect is performed. At the macroscopic scale, the evolution of stiffness reduction is determined for RO, HO-90° and HO-0° samples under quasi-static loading in order to emphasize the influence of fiber orientation. On the other hand, for RO samples, the microscopic damage propagation has been quantitatively related to its consequence on the macroscopic stiffness reduction. This quantitative analysis has been especially focused on the fiber-matrix interface mechanism which has been demonstrated in the previous section to be the predominant damage mechanism for A-SMC. The anisotropic strain rate effect on the fiber-matrix interface decohesion have been also studied through the comparison between damage threshold and kinetic measured for several fiber orientations chosen in RO samples.

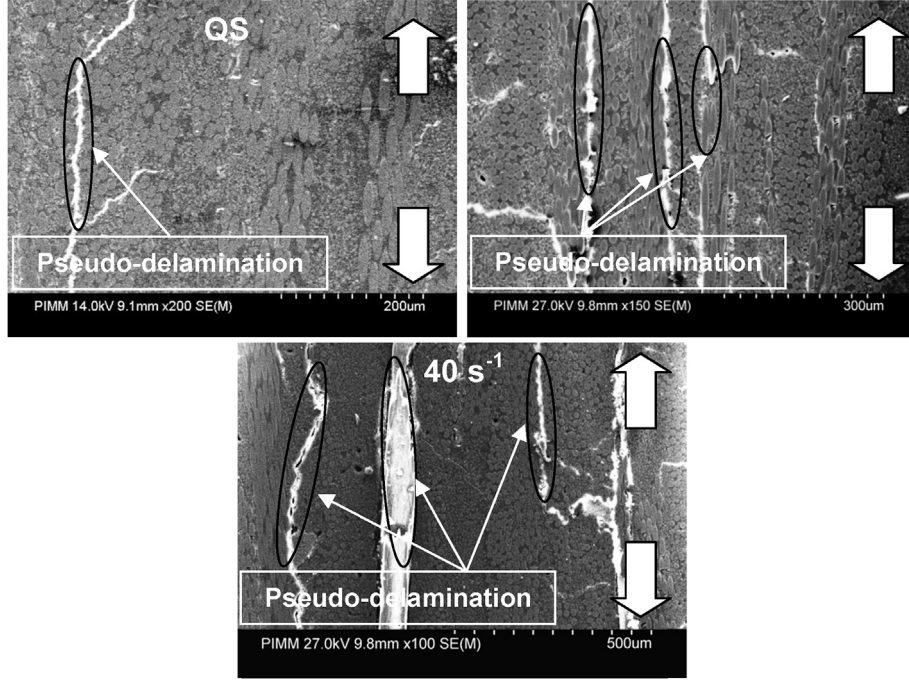


Fig. 10. Pseudo-delamination phenomenon at microscopic scale.

3.3.1. Damage indicators

Stiffness reduction is an appropriate macroscopic damage indicator to define damage development in short fiber reinforced composite materials [4–6]. In the case of tensile loading, one can define a macroscopic damage variable as [37]:

$$D_{\text{macro}} = 1 - \frac{E^D}{E^0} \quad (1)$$

E_0 and E_D are the Young's modulus of virgin and damaged material, respectively.

On the other hand, damage accumulation can be characterized in SMC composites by several elementary failure mechanisms such as matrix cracking, fiber breakage, debonding at the fiber-matrix interface and pseudo-delamination [4–6]. At microscopic scale, the stiffness reduction related to evolution of the micro-cracks density, the threshold and the kinetics of the cracks growth were demonstrated [12]. The damage mechanisms at the microscopic scale have been identified by means of SEM micrographs observations achieved upon polished specimen surfaces in the previous section. The evolution of the fiber-matrix damage mechanism can be quantitatively described by a local variable as [4–6]:

$$d_{\text{micro}} = \frac{f_d}{f_v} \quad (2)$$

Where f_d is the volume fraction of debonded fibers and f_v is the fiber volume content in the Representative Elementary Volume (REV). d_{micro} can also be defined as the debonded fibers proportion which is measured directly on the SEM micrographs by counting the number of fiber presenting an interface failure inside a bundle. Moreover, in order to study the influence of the fiber orientation on the damage strain rate effect, one can define the parameter $d(\theta)$ as follows [12]:

$$d_\theta = \frac{f_d^\theta}{f_\theta} \quad (3)$$

Where f_d^θ and f_θ are the volume fraction (or number) of the θ° oriented debonded fibers and the fibers volume content (or total number of fiber contained inside the bundle which is about 250) oriented at θ° , respectively.

3.3.2. Macroscopic scale

3.3.2.1. Quasi-static loading: effect of fiber orientation distribution. Fig. 11 shows the evolution of the macroscopic damage parameter, D , under quasi-static loading-unloading tensile test as a function of applied stress. It should be indicated that, for each microstructure, several tests (at least 3) were performed and the results have been reported in this figure in such a way that at least 15 points have been measured until the very last stages just before failure. One can note that in the case of HO-0° sample, the values of macroscopic damage parameter remains very low. This confirms that interface failure remains limited leading to a relative linear behavior as seen in Fig. 5(a) while pseudo-delamination is favored.

It should be noticed that HO-90° damage kinetic is higher than that of RO. This is essentially due to the fact that more fiber-matrix

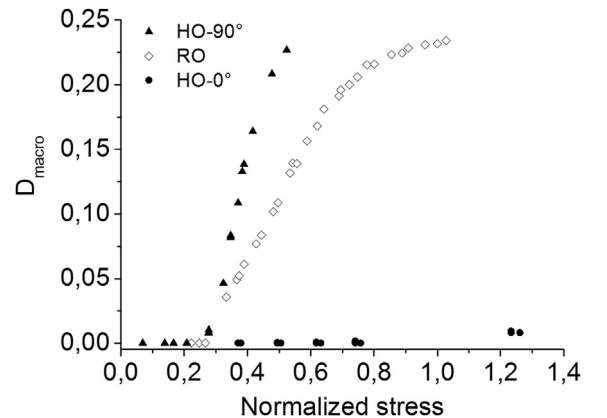


Fig. 11. Macroscopic damage evolution vs. applied stress for RO, HO-0° and HO-90° samples (Normalized value = current value/average ultimate stress (σ_r) value obtained for quasi-static tests performed on RO-A-SMC).

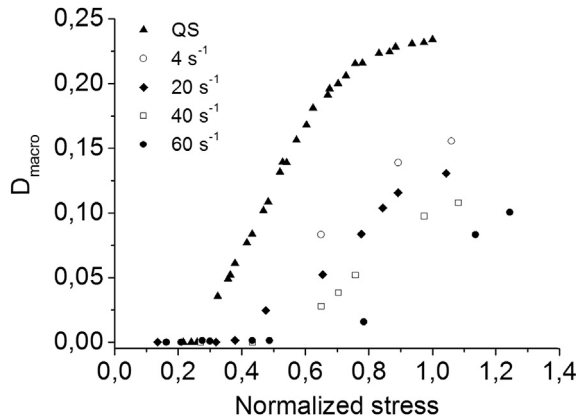


Fig. 12. Macroscopic damage evolution versus applied stress for different strain rates (Normalized value = current value/average ultimate stress (σ_r) value obtained for quasi-static tests performed on RO-A-SMC).

decohesions are involved in the case of HO-90° samples. On the other hand, one can also observe for RO samples an altered slope of the curve (from $D = 0.18$) indicating the saturation of the fiber-matrix interface failure occurring together with the beginning of the propagation of transverse cracks into the matrix. Finally, the critical value of D at failure for these two microstructures appears to be of the same order of magnitude which indicates a similar state of damage.

3.3.2.2. Effect of strain rate for RO samples. Experimental findings from Interrupted tensile tests (Fig. 12) performed at five different strain rates values varying from quasi-static (QS) to 60 s^{-1} confirm that strain rate increase leads to a delayed macroscopic damage initiation. Indeed, macroscopic loss of stiffness begins at a stress level of $0.30 \sigma_r$ in the case quasi-static tensile test whereas for a strain rate of 60 s^{-1} , the first stiffness reduction appears around a stress of about $0.60 \sigma_r$ which corresponds to a 100% augmentation of the damage threshold. Moreover, it should be indicated that the damage kinetic is more than three times reduced as the strain rate increases from quasi-static to 60 s^{-1} .

3.3.3. Microscopic scale

In order to understand the physical origin of the damage delay described in the previous sections, experimental investigations at the microscopic scale have been performed in order to identifying the corresponding damage mechanisms, their threshold and kinetic. Fig. 13 illustrates the global microscopic damage parameter

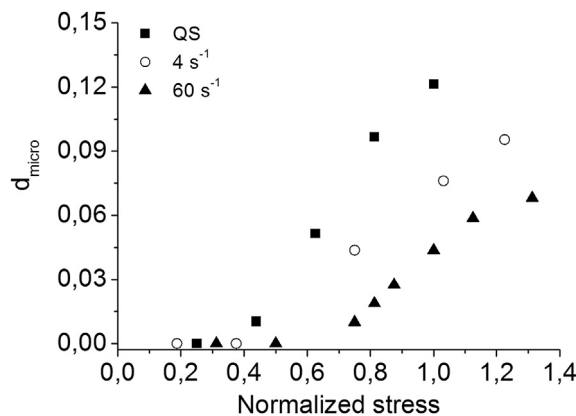


Fig. 13. Global microscopic damage evolution versus strain rate (Normalized value = current value/average ultimate stress (σ_r) value obtained for quasi-static tests performed on RO-A-SMC).

(d_{micro}) evolution as a function of the applied stress, previously defined in equation (2), for Randomly Oriented (RO) samples at different strain rates ranging from quasi-static to 40 s^{-1} .

In accordance with the macroscopic damage indicator evolution, the damage threshold analyzed at the microscopic scale is shifted to higher values and the damage growth is reduced when increasing strain rate. These aspects account on the well known visco-damage effect described in previous papers [4–7].

3.3.3.1. Anisotropic strain rate effects on the fiber-matrix interface decohesion. In the following, the influence of fiber orientation on interfacial micro-cracks density evolution is discussed. Different families of fiber orientation bundles were selected at microscopic scale and their damage evolution were investigated at each defined applied stress and strain rates. Note that the 30° family (respectively 45° and 90°) results presented in Fig. 14 correspond to the

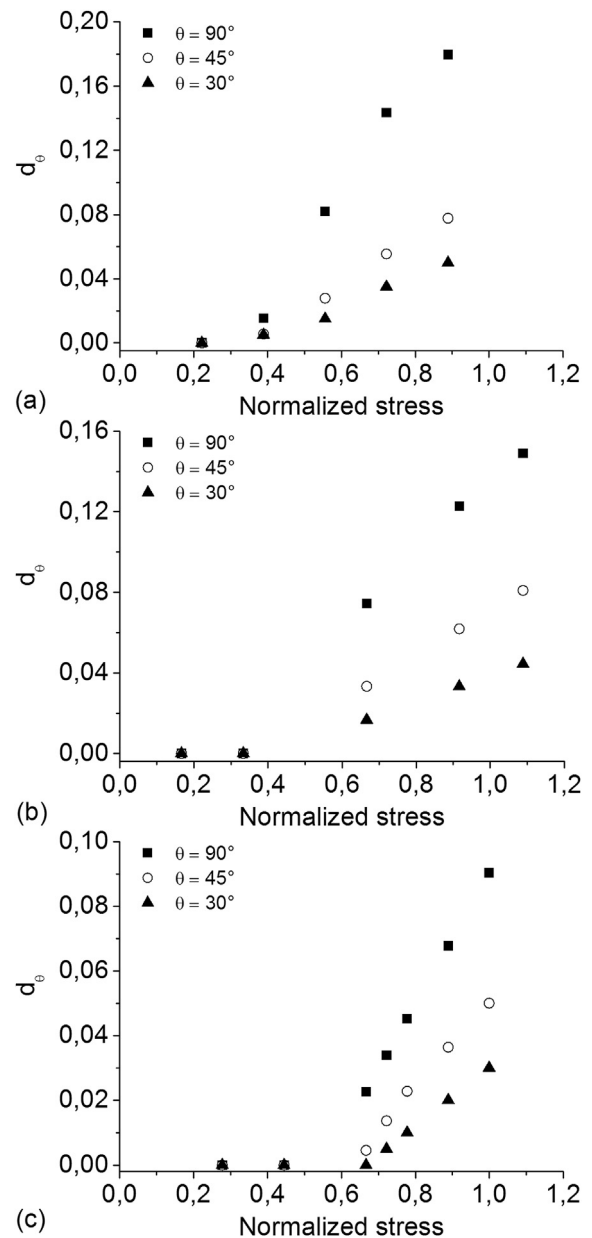


Fig. 14. Evolution of d_0 as a function of applied stress; (a) Quasi-static, (b) Strain rate of 4 s^{-1} and (c) Strain rate of 40 s^{-1} (Normalized value = current value/average ultimate stress (σ_r) value obtained for quasi-static tests performed on RO-A-SMC).

averaged crack density evolution obtained for fiber orientation ranging from 20° to 30° (respectively from 35° to 55° and from 80° to 90°).

Fig. 14 shows the evolution of the fiber-matrix interface local damage indicator for each specified orientation family (d_0), at strain rates varying from quasi-static to 40 s⁻¹. One can note that independently of applied strain rate, when increasing fiber orientation, damage threshold stress decreases while the damage kinetic increases.

Fiber-matrix decohesion can occur when a combination of a local ultimate normal and shear stress are reached on the interface [4]. 45° oriented fibers are submitted to higher interfacial shear stresses while fiber-matrix interface of 90° oriented fibers fails under a pure normal stress.

In Fig. 15, the evolution of the relative damage threshold and kinetic (determined by the slope of between the density evolution curve) have been plotted as a function of the strain rate for the three defined fiber orientations. A noticeable local anisotropic strain rate effect can be pointed out. Indeed, this figure shows that when the fibers are oriented in the tensile direction, the damage onset due to increasing strain rate is favored while the damage kinetic is altered. These coupled effect of strain rate and orientation on the fiber-matrix interface failure will be discussed in the next section.

4. Viscous nature of the microscopic damage

In this section, the whole experimental results described above are used to propose an interpretation of the origin of the strain rate effect on damage of A-SMC composites. Obviously, interactions between microscopic and macroscopic scale are considered. Moreover, it is shown that to get a thorough understanding of the strain rate dependent damage behavior of A-SMC, it is also necessary to analyze the influence of the deformation mechanisms occurring at the polymer chains scale. Note that the multi-scale analysis proposed hereafter is also suitable for many short fiber reinforced composites.

4.1. Characteristic times and relaxation times

In order to understand the origin of the viscous nature of damage accumulation, one can define a specific characteristic time which is required for a local damage or deformation mechanism to occur. Indeed, this characteristic time is related to the viscoelastic

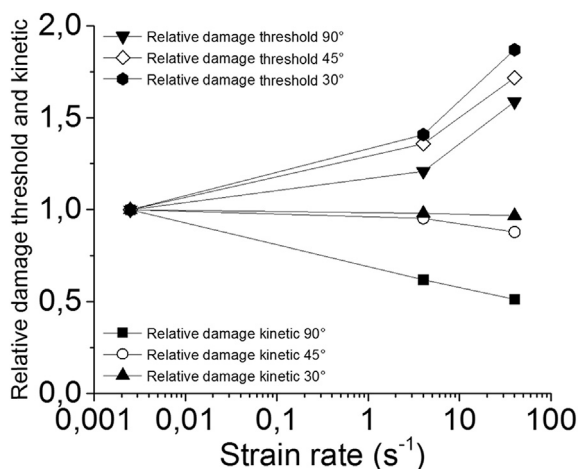


Fig. 15. Evolution of the relative damage threshold and kinetic as a function of the strain rate.

behavior of the matrix or fiber/matrix interface-interphase or, more precisely, to the relaxation time of the constitutive polymers of the latter. These relaxation times are related to the mobility of the molecular chains constituting the matrix and the fiber-matrix interface (on which depend adhesion properties). The relaxation time of a polymer is defined as $\tau = \eta/E$ where η and E are viscosity and modulus, respectively. It is important to remember that these two parameters are intrinsic properties of polymers and are directly related to the adhesion force between molecular chains and their mobility. Then, the relative values of the different relaxation times (matrix and fiber-matrix interface) versus the loading rate determine how the damage will develop over time. Indeed, the value of the imposed strain rate determine a characteristic time of the loading.

4.2. Origin of the strain rate effect on damage threshold, kinetic and diffusion

Under quasi-static loading, the local damage characteristic times related to the relaxation times of each constitutive polymer (matrix and fiber-matrix interface) are far below that of the imposed loading characteristic time. Under such conditions, damage can easily occur in a diffuse manner. In fact, when damage occurs on one location, sufficient time remains for the material to generate other damage events on other locations. Consequently, damage is systematically delocalized to other sites. This leads to foster diffuse damage. As a result, low threshold and high kinetic of local degradation are observed. When one type of mechanism get saturated, another one can take place as it can be seen on Fig. 12 for quasi-static curve (see the altered slope from $D = 0.18$ highlighting a saturation of the fiber-matrix decohesion together with the beginning of the micro-cracks propagation from the interfaces to the matrix).

On the other hand, when increasing strain rate, the characteristic loading time can reach the same order of magnitude than the required time for local damage mechanisms to occur (which is related to matrix and/or fiber-matrix interface relaxation times). At these speeds, polymer chains mobility is not sufficient to allow easy local deformation. Thus, local deformation and damage initiation require more energy. On one hand, this leads to shift damage threshold to higher values of applied stress and to reduce the local degradation kinetic on the other hand. Moreover, under rapid loading, relatively high value of local relaxation times (matrix and/or fiber-matrix interface) versus strain rate do not allow the accommodation of the deformation through systematic damage delocalization. Consequently, one can observe an easier concentrate accumulation of micro-cracks which can rapidly lead to more localized failure when increasing strain rate.

4.3. Influence of the deformation mechanisms at the polymer chains scale on fiber-matrix interface damage rate

In the case of A-SMC composites, it is of first importance to understand the origin of the strain rate effect on the fiber-matrix interface failure which appears to be the predominant damage mechanism and the more sensitive to strain rate effect. Indeed, the mobility of the macromolecules near to the surface of the fibers (interface or interphase) may be affected by the rigidity of the fibers. So, one may suppose that the relative values of τ and τ' , corresponding to the relaxation times relative to the molecular mobility respectively far and near to the fibers can play an important role in the fiber-matrix interface damage delay and altered damage kinetic observed when increasing strain rate. Actually, because of lower crosslinking density of the matrix around the fibers, because of chemical bonds between matrix and coupling

agent and finally because of the high rigidity of this later (Fig. 16), τ' is generally higher than τ . Thus, when loading rate increases, the mobility of the macromolecules near to the interface is not sufficient to accommodate the deformation. Therefore, the high sensitivity to strain rate observed especially for fiber-matrix interface damage can be interpreted as a consequence of the higher value of τ' .

Moreover, by increasing the temperature, the relaxation time of polymers generally increases. Moreover, under high strain rate loading, self-heating probably occurs at local scale (matrix and fiber-matrix interface). Thus, because of lower crosslinking and higher local self-heating due to strain localization at interface, this effect is more significant for the macromolecules near to the fibers.

4.4. Microstructure and local anisotropic strain rate effect on fiber-matrix interface damage

Moreover, in the previous section (Figs. 14 and 15), it has been shown that, at the fiber-matrix interface scale, the ultimate normal stress is more sensitive to strain rate than the ultimate interface shear stress. Indeed, under high strain rate, normal interface failure requires more energy. In fact, when the stress is normal, at local scale, mostly the bonds between matrix and coupling agent (at the surface of fibers) will be under loading; while for shear stress, both matrix and bonds at interface will be submitted to the local load. It is important to precise that generally the chemical cross-linking bonds are more important than the bonds between matrix and fibers. Consequently, at a given strain rate, normal failure at the fiber-matrix interface is always favored compared to shear mode failure (See damage threshold evolution on Fig. 15). Thus, transversely oriented fibers and high strain rate will contribute to lower kinetic of damage accumulation. This leads to a prompt loss of stiffness in the case of HO-90° samples, a moderate one for RO samples and to a very limited one for HO-0° samples (see Fig. 11).

4.5. Strain rate and fiber orientation effects on pseudo-delamination

On the other hand, it has been shown that high strain rate and oriented fibers favor pseudo-delamination. This mechanism occurring prior to the final failure is always preceded by the propagation of localized micro-cracks coming from neighbor's interfaces decohesion inside the bundles into the matrix until another bundle.

The multi-scale damage analysis showed that the fiber-matrix interface damage is limited for a high oriented microstructure. On the other hand, the strain rate effect appears to be predominantly due to the local damage at the most miss-oriented fiber interface. Thus, in the case of highly oriented microstructure, interfacial damage and strain rate effect on its accumulation remain limited.

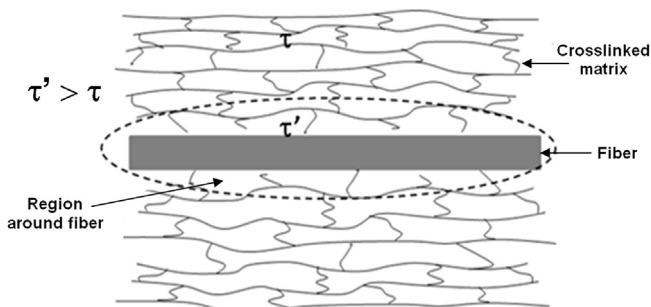


Fig. 16. Polymer structure near and far from the interface and related relaxation times.

Consequently, high strain rate and orientation together contribute to a rapid saturation of the fiber-matrix interface damage accumulation and a prompt propagation of the micro-cracks from the interface into the matrix between the bundles of fibers. Consequently, especially for HO-0° samples submitted to high applied strain rate, fiber-matrix interface damage accumulation is altered while damage onset increases and pseudo-delamination is favored.

5. Conclusion

In automotive industry, a new formulation of high glass fiber content SMC is used for structural parts submitted to crash events. These Advanced Sheet Molding Compound composites must be able to absorb sufficient energy during a crash event in order to assure safety of the passengers. To this aim, the capability of the constitutive material to develop a non linear behavior through damage accumulation is a central purpose of study.

In this paper, a multi-scale experimental analysis of the damage behavior of an A-SMC composite has been performed. A specific device has been developed in order to be able to characterize at both microscopic and macroscopic scales, the evolution of the damage accumulation at quasi-static and high applied strain rates. Interrupted tensile test technique has been used in order to determine, for several microstructure configurations (RO, HO-90° and HO-0°), qualitatively and quantitatively the damage effect during high speed tensile loading ranging from quasi-static to 60 s⁻¹. Quantitatively, the SEM analysis coupled to IDTT led to the following conclusions:

- Fiber-matrix interface failure appears to be the predominant mechanism,
- Matrix micro-cracking coming from the propagation of the interface micro-cracks into the matrix located between the bundles of fibers is favored at high strain rates,
- Pseudo-delamination between the bundles of fibers coupled with the matrix micro-cracking described above always occurs prior to the final failure and is favored by high strain rate and orientation of the fibers in the loading direction.

Microscopic and macroscopic damage indicators have been proposed and well correlated each other for various microstructures and strain rates. The evolution of the fiber-matrix interface cracks density has been measured as a function of applied strain rate ranging from quasi-static to 40 s⁻¹ for Randomly Oriented samples. An increase of the strain rate leads to an augmentation of the damage threshold together with a diminution of the damage accumulation kinetic and a less diffuse spatial distribution of the micro-cracks. Moreover, in order to emphasize the effect of the fiber orientation, an analysis of the interface damage accumulation have been performed on 30°, 45° and 90° oriented bundles of fibers statistically chosen on RO samples micrographs. It has been shown that the strain rate effect on microscopic damage accumulation is mostly due to the specific sensitivity of the ultimate normal stress at the interface. The latter leads to a more sensitive strain rate effect for RO and HO-90° A-SMC samples observed at the macroscopic scale.

Finally, the origin of the viscous nature of the microscopic damage has been discussed and correlated to the macroscopic damage thresholds delays and damage kinetics as a function of the microstructure and the strain rate. Specific considerations at the polymer chains scale allow proposing a consistent interpretation of the origin and the nature of strain rate effect described in this study.

The multi-scale experimental analysis performed in this study led also to a deep understanding of the origin of the anisotropic elastic visco-damageable behavior of A-SMC composites and

constitutes a rich database for the development of further micro-mechanical modeling for A-SMC automotive structures submitted to crash events [27].

References

- [1] Sun L, Gibson RF, Gordaninejad F, Suhr J. Energy absorption capability of nanocomposites: a review. *Compos Sci Technol* 2009;69(14):2392–409.
- [2] Huang H, Talreja R. Numerical simulation of matrix micro-cracking in short fiber reinforced polymer composites: initiation and propagation. *Compos Sci Technol* 2006;66(15):2743–57.
- [3] Kun F, Zapperi S, Herrmann HJ. Damage in fiber bundle models. *Eur Phys J B - Condens Matter Complex Syst* 2000;17(2):269–79.
- [4] Fitoussi J, Bocquet M, Meraghni F. Effect of the matrix behavior on the damage of ethylene-propylene glass fiber reinforced composite subjected to high strain rate tension. *Compos Part B Eng* 2013;45(1):1181–91.
- [5] Fitoussi J, Meraghni F, Jendli Z, Hug G, Baptiste D. Experimental methodology for high strain-rates tensile behaviour analysis of polymer matrix composites. *Compos Sci Technol* 2005;65(14):2174–88.
- [6] Fitoussi J, Guo G, Baptiste D. A statistical micromechanical model of anisotropic damage for S.M.C. composites. *Compos Sci Technol* 1998;58(5):759–63.
- [7] Shirinbayan M, Fitoussi J, Meraghni F, Surowiec B, Bocquet M, Tcharkhtchi A. High strain rate visco-damageable behavior of Advanced Sheet Molding Compound (A-SMC) under tension. *Compos Part B Eng* 2015;3670(82):30–41.
- [8] Farley GL. Energy absorption in composite structures. *J Compos Mater* 1983;17:267–79.
- [9] Jacob GC, Fellers JF, Simunovic S, Starbuck JM. Energy absorption in polymer composites for automotive crashworthiness. *J Compos Mater* 2002;36(7): 813–50.
- [10] Lee HK, Simunovic S. A damage mechanics model of crack-weakened, chopped fiber composites under impact loading. *Compos Part B Eng* 2002;33(1): 25–34.
- [11] Okoli OI. The effects of strain rate and failure modes on the failure energy of fibre reinforced composites. *Compos Struct* 2001;54(2):299–303.
- [12] Jendli Z, Fitoussi J, Meraghni F, Baptiste D. Anisotropic strain rate effects on the fibre-matrix interface decohesion in sheet moulding compound composites. *Compos Sci Technol* 2005;65(3–4):387–93.
- [13] Baste S, Gérard A. Evaluation of anisotropic damage in composite materials. *Eval anisotropic damage Compos Mater* 1994;3:2025–32.
- [14] Achour N, Chatzigeorgiou G, Meraghni F, Chemisky Y, Fitoussi J. Implicit implementation and consistent tangent modulus of a viscoplastic model for polymers. *Int J Mech Sci* 2015;103:297–305.
- [15] Kästner M, Obst M, Brummund J, Thielsch K, Ulbricht V. Inelastic material behavior of polymers-experimental characterization, formulation and implementation of a material model. *Mech Mater* 2012;52:40–57.
- [16] Kim J, Muliiana A. A time-integration method for the viscoelastic-viscoplastic analyses of polymers and finite element implementation. *Int J Numer Methods Eng* 2009;79(5):550–75.
- [17] Kweon S, Benzerga A. Finite element implementation of a macromolecular viscoplastic polymer model. *Int J Numer Methods Eng* 2013;94(10):895–919.
- [18] Patel BP, Gupta AK. An investigation on nonlocal continuum damage models for composite laminated panels. *Compos Part B Eng* 2014;60:485–94.
- [19] Bere P, Berce P, Nemes O. Phenomenological fracture model for biaxial fibre reinforced composites. *Compos Part B Eng* 2012;43(5):2237–43.
- [20] Tanaka K, Mori T. The hardening of crystals by non-deforming particles and fibres. *Acta Metall* 1970;18(8):931–41.
- [21] Morozov EV, Morozov KE, Selvarajalu V. Damage model development for SMC composites. *Compos Struct* 2003;62:373–8.
- [22] Lacy TE, MacDowell DL, Talreja R. Gradient concepts for evolution of damage. *Mech Mater* 1999;31(12):831–60.
- [23] Shao JF, Rudnicki JW. A microcrack-based continuous damage model for brittle geomaterials. *Mech Mater* 2000;32:607–19.
- [24] Nedjar B. Elastoplastic-damage modelling including the gradient of damage: formulation and computational aspects. *Int J Solids Struct* 2001;38(30–31): 5421–51.
- [25] Askes H, Sluys LJ. Explicit and implicit gradient series in damage mechanics. *Eur J Mech Solids* 2002;21(3):379–90.
- [26] Shao JF, Rudnicki JW. A microcrack-based continuous damage model for brittle geomaterials. *Mech Mater* 2000;32:607–19.
- [27] Jendli Z, Meraghni F, Fitoussi J, Baptiste D. Multi-scales modeling of dynamic behaviour for discontinuous fibre SMC composites. *Compos Sci Technol* 2009;69(1):97–103.
- [28] Jendli Z, Meraghni F, Fitoussi J, Baptiste D. Micromechanical analysis of strain rate effect on damage evolution in sheet molding compound composites. *Compos Part A Appl Sci Manuf* 2004;35(7–8):779–85.
- [29] Arif MF, Saintier N, Meraghni F, Fitoussi J, Chemisky Y, Robert G. Multiscale fatigue damage characterization in short glass fiber reinforced polyamide-6. *Compos Part B Eng* 2014;61:55–65.
- [30] Aymerich F, Meili S. Damage assessment in an SMC composite by means of ultrasonic techniques. *NDT.NET* 1999;4(3).
- [31] Le TH, Dumont PJJ, Orgéas L, Favier D, Salvo L, Boller E. X-ray phase contrast microtomography for the analysis of the fibrous microstructure of SMC composites. *Compos Part A Appl Sci Manuf* 2008;39(1):91–103.
- [32] Feuillade V, Bergeret A, Quantin J, Crespy A. Characterisation of glass fibres used in automotive industry for SMC body panels. *Compos Part A Appl Sci Manuf* 2006;37(10):1536–44.
- [33] Bussiba A, Kupiec M, Ifergane S, Piat R, Böhlke T. Damage evolution and fracture events sequence in various composites by acoustic emission technique. *Compos Sci Technol* 2008;68(5):1144–55.
- [34] Derrien K, Baptiste D, Guedra-Degeorges D, Foulquier J. Multiscale modeling of the damaged plastic behavior and failure of Al/SiCp composites. *Int J Plasticity* 1999;15(6):667–85.
- [35] Meraghni F, Benzeggagh ML. Micromechanical modelling of matrix degradation in randomly oriented discontinuous-fibre composites. *Compos Sci Technol* 1995;55(2):171–86.
- [36] Lataillade JL, Delaet M, Collombet F, Wolff C. Effects of the intralaminar shear loading rate on the damage of multi-ply composites. *Int J Impact Eng* 1996;18(6):679–99.
- [37] Krajcinovic D, Mastilovic S. Some fundamental issues of damage mechanics. *Mech Mater* 1995;21(3):217–30.